

## THIN FILM SUPERPLASTIC FORMING MODEL FOR NANOSCALE BULK METALLIC GLASS FORMING

Catherine Mros

Mechanical Engineering Department  
University of New Hampshire  
33 College Road, Durham, NH 03824  
cbu9@unh.edu

Kavic Rason

Mechanical Engineering Department  
University of New Hampshire  
33 College Road, Durham, NH 03824  
rws6@unh.edu

Brad Kinsey

Mechanical Engineering Department  
University of New Hampshire  
33 College Road, Durham, NH 03824  
bkinsey@unh.edu

### ABSTRACT

Geometrically complex, high aspect ratio microstructures have been successfully formed in Bulk Metallic Glass (BMG) via superplastic forming against silicon dies [1-3]. Although nanoscale features have been created in a similar fashion, there exists a demand to develop these metallic nanostructures into high aspect ratio nanostructures with controlled geometries. In past research a process model was created to predict the achievable nanoscale feature sizes and aspect ratios through a flow model [4]. The flow model assumes force equilibrium with a viscous term to account for the required force to produce flow and a capillary pressure term required to overcome surface effects which are significant at the nanoscale. In this paper, a thin film model to predict the pressure distribution across the BMG during the forming process when it is in the supercooled liquid state is presented. Silicon molds with various nanostructures were produced using Deep Reactive Ion Etching to achieve high aspect ratio dies over a relatively large area in order to validate these models.

### INTRODUCTION

Technological advances in nanotechnology are fueling a need for high rate nanomanufacturing processes. Current processes at this size scale are time intensive and costly. For example, thin film deposition, a process by which atoms are deposited onto a substrate one layer at a time [5], is precise, yet slow and costly. Another more traditional process is integrated circuit lithography. Again this process produces high quality parts but has high costs due to the clean room space and nanofabrication equipment required. Also features are limited to 2.5 dimensions and certain materials.

Therefore there is a need for mass producing precise patterned nanoscale features at low costs and with durable materials. The nanoforming process is an inexpensive mass production manufacturing process that can produce Bulk Metallic Glass (BMG) components. Geometrically complex,

high aspect ratio microstructures have been successfully replicated into Zirconium based BMGs, commercially known as the Vitreloy series of alloys from LiquidMetal Technologies [6], by molding them against patterned Silicon or SiO<sub>2</sub> substrates [1,2]. Although there are several types of bulk metallic glass, the one used in this paper is Zr<sub>44</sub>Be<sub>25</sub>Ti<sub>11</sub>Cu<sub>10</sub>Ni<sub>10</sub>, or Vitreloy 1b. This particular alloy is well suited for filling high aspect ratio, complex features and withstanding high temperatures for molding processes [1]. The property that allows BMG to be formed at the nanoscale is that it has an amorphous structure, i.e., it can contain no metallic grains unlike typical polycrystalline metals. This causes it to be homogenous and isotropic at the atomic scale. Further understanding of this material can be obtained through a time temperature transition (TTT) diagram as shown in figure 1.

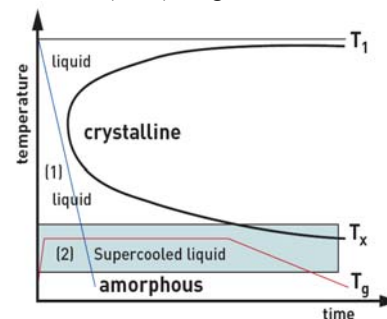


Figure 1: Schematic TTT diagram illustrating rapid quench casting of a BMG from its molten state (1) and a molding process of the material in its supercooled liquid state (2) [1].

As long as the forming process stays to the left of the TTT curve the material will not crystallize. If the process causes the BMG to be heated for too long, the glass will start to form crystals and become brittle. Preventing crystallization is ideal, as the BMG remains strong and has a high impact resistance, as well as high corrosion resistance at elevated temperatures. This

causes it to be a good material for use as a mold for other processes such as injection molding.

In this paper, a theoretical model for the pressure distribution within the BMG during the superplastic forming process is presented. A more robust process and new molds with high aspect ratio features were created. Future experiments will be used to determine the highest achievable aspect ratio and the pressure distribution within the BMG to compare with model results. Insight into these values will allow high rate nanomanufacturing to occur, as multiple molds will be able to be fabricated simultaneously.

## THEORETICAL MODEL

It is the pressure within the BMG that is directly responsible for driving the nanomolding process (not to be confused with the constant pressure applied to the mold chip). Therefore an understanding of the pressure distribution across the BMG during the molding process is essential. In a macroscopic sense, the molding process can be modeled as a squeezed viscous thin film since the supercooled liquid BMG is known to behave as an incompressible, Newtonian fluid at elevated temperatures [4]. This approach is typically employed when the film thickness is much smaller than the film width, which is true in this case (i.e., a mold of 10mm x 10mm with an initial BMG thickness of approximately 1 mm which rapidly decreases as the molding process progresses). Such a model neglects the small variation in pressure across the thickness of the film. Additionally, although the flow is not at a steady state, inertial effects within the flowing film are also neglected by a creeping flow assumption, which is supported by the very low characteristic Reynolds Number of the flow which has been calculated at the end of this section. This Reynolds Number calculation is performed for the macroscopic flow of material as a thin film.

A typical molding process consists of three distinct phases. First the film is heated to a constant temperature (e.g., 450°C) by contact with the heated platens (see Fig. 2a.). It is then squeezed by a constant force applied equally by the upper platen and the nanopatterned molding chip (see Fig.2b.). Finally, once the molding process is completed, the film is rapidly quenched back to room temperature and the applied pressure is removed (see Fig. 2c.). The process produces a thin film of BMG between the mold and the platen.

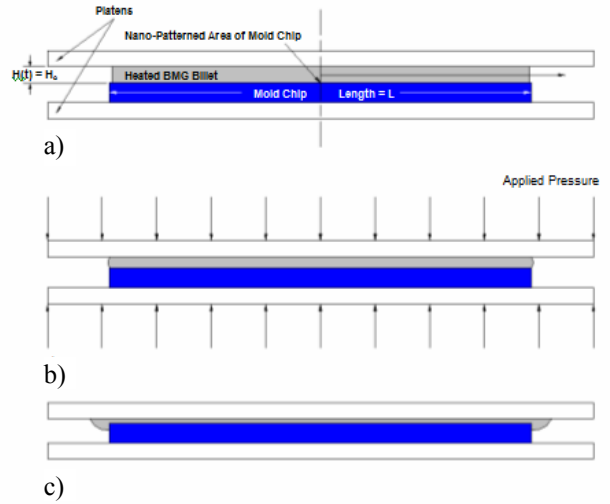


Figure 2: Macroscopic schematic of the molding process a) initially, b) as the BMG is squeezed and flows laterally, and c) with the final thin film of BMG between the mold and the platen.

The equations for the squeezed, thin film model follow. Simplification of the Navier-Stokes equations and the continuity condition for a squeezed viscous film yields the following expression

$$\frac{1}{\mu} \frac{d}{dx} \left( H^3 \frac{dp}{dx} \right) = -12 \frac{dH}{dt} \quad (1)$$

where  $\mu$  is the viscosity,  $x$  is the lateral distance from the center of the mold,  $H$  is the film thickness (see Fig. 2), and  $p$  is the local pressure within the thin film. This equation is commonly known as the Reynolds Equation for a squeezed film [7]. Taking advantage of symmetry, this expression is integrated from the center of the mold ( $x=0$ ) to the edge of the squeezed film ( $x=L/2$ , where  $L$  is the total width of the mold). This yields the following expression for the lateral pressure gradient in the film of BMG.

$$\frac{dp}{dx} = -\frac{12\mu}{H^3} \frac{dH}{dt} x \quad (2)$$

where the constant of integration is found to be zero by applying the symmetry boundary condition at the center of the chip

$$\left. \frac{dp}{dx} \right|_{x=0} = 0 \quad (3)$$

Integrating a second time and applying the free surface condition at the edge of the chip

$$p(L/2) = 0 \quad (4)$$

yields the following expression

$$p_{BMG}(x,t) = -\frac{6\mu}{H(t)^3} \frac{dH}{dt} \left( x^2 - \frac{L^2}{4} \right) \quad (5)$$

Thus, the pressure distribution in the film is now defined as a function of position and time. However, this expression is not directly useful, as the film thickness function is still undefined. It is therefore necessary to equate the average applied pressure with the undefined film pressure as depicted in Fig. 3.

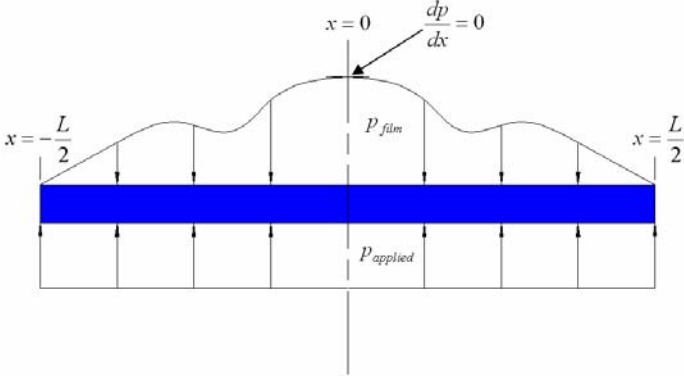


Figure 3: Schematic of molding process including definitions of parameters.

Neglecting inertial effects and once again taking advantage of symmetry, this condition may be expressed as

$$\int_0^{L/2} P_{applied} dx = \int_0^{L/2} P_{BMG} dx \quad (6)$$

where the film pressure is defined by Eq. 5 and the applied molding pressure is known to be constant with respect to time and location on the surface of the mold chip

$$P_{applied} = \frac{F}{A} = \frac{F}{L^2} \quad (7)$$

where the mold chip is square with a dimension of  $L$ . Therefore Eq. 6 becomes

$$\int_0^{L/2} \frac{F}{L^2} dx = \int_0^{L/2} \frac{6\mu}{H(t)^3} \frac{dH}{dt} \left( x^2 - \frac{L^2}{4} \right) dx \quad (8)$$

Performing this integration and rearranging yields the desired expression for the thinning rate of the squeezed film, as a function of the film viscosity and known molding system parameters

$$\frac{dH}{dt} = -\frac{F}{L^4 \mu} H^3 \quad (9)$$

Upon examination of this expression it is observed that the rate of film thinning *decreases* at a rate which is proportional to a reduction in film thickness cubed. Recall, that Eq. 5 states that the pressure within the film will *increase* at a rate which is proportional to a reduction in film thickness cubed. Therefore, substitution of Eq. 9 into Eq. 5 results in a cancellation of the effect of the thinning film thickness. Subsequently, all time dependence of the pressure within the thin film of BMG is removed, since the film thickness was the

only time dependent parameter in Eq. 5. For similar reasons, the effect of material viscosity also cancels out of the following expression.

$$p(x)|_{film} = -\frac{3F}{2L^2} \left[ \left( \frac{2x}{L} \right)^2 - 1 \right] \quad (10)$$

Finally, recognizing the applied molding pressure term in the above expression allows the equation to be re-written as

$$p(x)|_{film} = -\frac{3}{2} P_{applied} \left[ \left( \frac{2x}{L} \right)^2 - 1 \right] \quad (11)$$

This expression allows for the determination of the local pressure within the squeezed film of BMG as a function of the known applied molding pressure. A properly scaled representation of the squeezed, thin film pressure distribution is provided in Fig. 4.

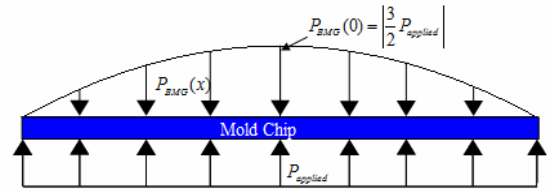


Figure 4: Predicted pressure distribution within the thin film of the BMG

Finally, the creeping flow assumption of the thin film model can be verified by calculation of the Reynolds Number, which is defined as

$$Re = \frac{UH\rho}{\mu} \quad (12)$$

where  $\rho$  is the mass density of the BMG and  $U$  is the lateral mean flow velocity of BMG, which may be calculated by conservation of mass and incompressibility (see Fig 5 and Eq. 13).

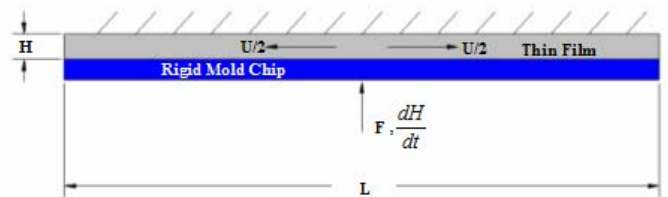


Figure 5: Schematic of material flow in the molding process.

$$\frac{U}{H} = \frac{dH/dt}{L} \quad (13)$$

Substitution of Eq. 13 into Eq. 12 allows the Reynolds number to be expressed as

$$\text{Re} = \frac{H^2 \rho}{\mu L} \frac{dH}{dt} \quad (14)$$

and substitution of Eq. 9 into this expression yields

$$\text{Re} = \frac{H^5 \rho F}{4 \mu^2 L^5} \quad (15)$$

Application of typical molding parameters (e.g.  $\mu$  equal to  $2 \times 10^7$  Pa/s,  $\rho$  equal to  $6100 \text{ kg/m}^3$ ,  $L$  equal to  $5 \text{ mm}$ ,  $H$  equal to  $1 \text{ mm}$ ,  $F$  equal to  $2000 \text{ N}$ ) to Eq. 15 results in a characteristic Reynolds number equal to  $7.63 \times 10^{-14}$  which strongly supports the creeping flow assumption.

Unfortunately, the limited aspect ratios of the mold features in past experiments were inadequate for validation of these calculations [4]. High aspect ratio molds from silicon via Deep Reactive Ion Etching (DRIE) were created to address this limitation. Experimentation with these molds will allow for direct validation of both the thin film and nanofluidic molding models.

## EXPERIMENTAL APPROACH

In order to test the validity of the thin film model and a nanomolding model developed in past work [8] an existing experimental setup was modified and new molds were created. Custom fixturing was installed on a model 1350 Instron Mechanical testing machine to allow for precise heating and subsequent rapid quenching of molded specimens. See Fig. 6 for a schematic of the system, and Fig. 7 for a picture of the experimental set-up.

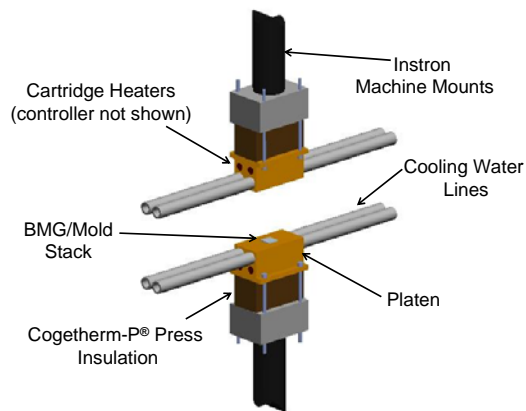


Figure 6: Schematic of experimental set-up including components for heating and cooling.

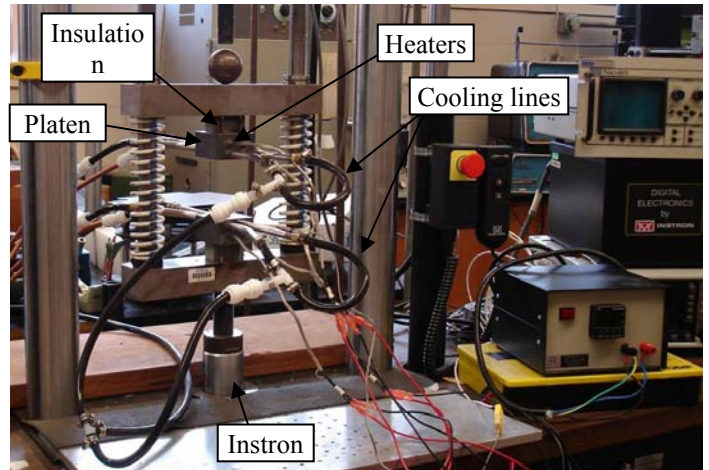


Figure 7: Picture of the experimental set-up.

The BMG must be rapidly quenched while pressure is still being applied in order to insure that the material does not flow back out of the nanoscale mold features and to keep the BMG from crystallizing. After some experimentation the molding parameters were determined to be  $450^\circ\text{C}$ ,  $100\text{MPa}$  for approximately 35sec.

New Si molds were fabricated containing high aspect ratio (height/width) features. These new molds will be used to validate the theoretical models.

Two sizes of mold chips were created via electron beam lithography and deep reactive ion etching with ZEP used as the resist. The first size chip is  $10\text{mm} \times 10\text{mm}$ . These chips have 35 sets of features on them arranged as shown in Fig. 8a. Each set of features on the  $10\text{mm} \times 10\text{mm}$  chips consisted of 16 trenches  $400\text{nm}$  wide  $\times$  approximately  $800\text{nm}$  apart, a triangular trench of  $3\mu\text{m}$  at its widest point, and 24 trenches  $200\text{nm}$  wide  $\times$  approximately  $1\mu\text{m}$  apart, all of which were  $110\mu\text{m}$  in length. These features are shown in the SEM image of Fig. 9.

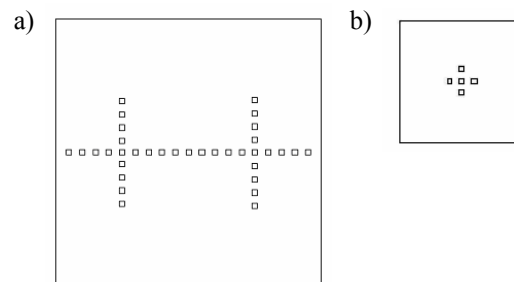


Figure 8: a) Arrangement of feature sets on the  $10\text{mm} \times 10\text{mm}$  chips and b) Arrangement of feature sets on the  $5\text{mm} \times 5\text{mm}$  chips.

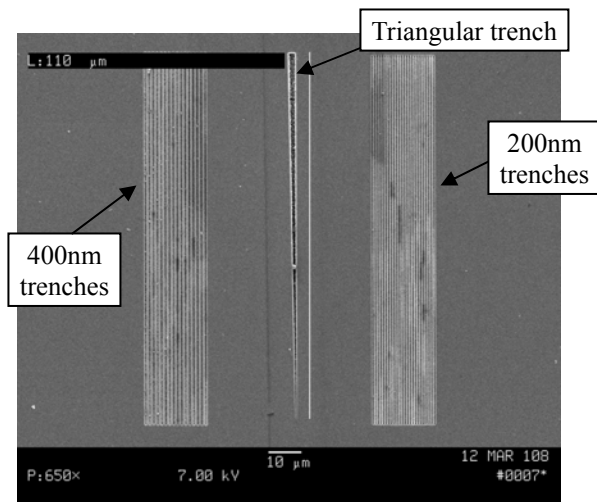


Figure 9: SEM image of 10mm x 10mm chip features

The second size chip is 5mm x 5mm. Each chip contains 5 sets of features arranged as shown in Fig. 8b with multiple sets of varied sized trenches and spacing. They also contain a triangular trench (see Fig. 11a) of the same measurements on the 10mm x 10mm chips. Last there are a set of holes as the ones shown in Fig. 11b. The arrangement of the feature types on the 5mm x 5mm mold is shown in figure 10.

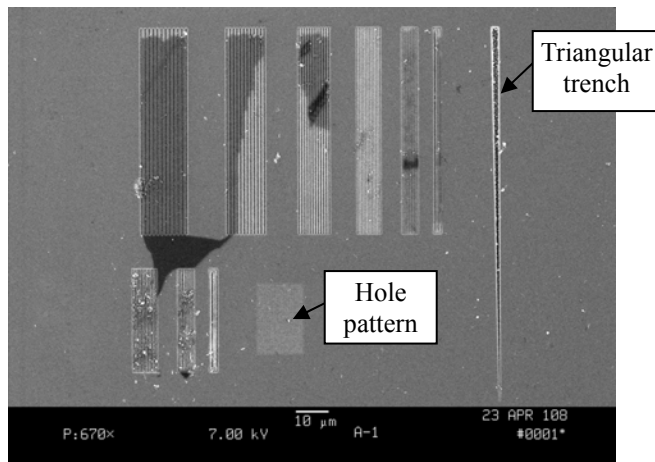


Figure 10: SEM image of 5mm x 5mm chip features

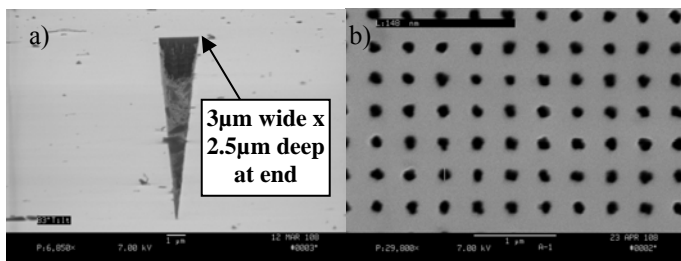


Figure 11: a) SEM image of triangular trench feature on both size chips and b) SEM image of hole features on 5mm x 5mm size chips.

The depths on both sizes of chips vary from approximately 550nm to approximately 750nm. This creates aspect ratios ranging from 1.8 to 3 (see Fig. 12).

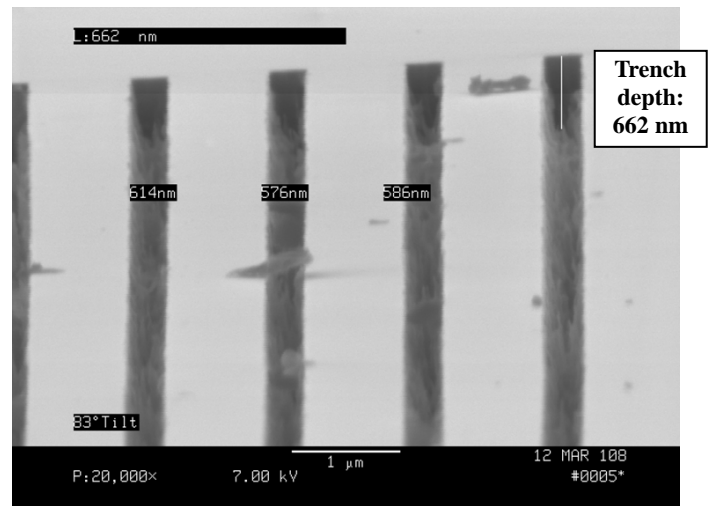


Figure 12: SEM image of sample set of trench features

## DISCUSSION

The two sizes of mold chips will be used to validate the two theoretical models, the thin film model discussed in this paper and the nano-molding model [8]. The 10mm x 10mm chips will be used to determine the pressure distribution across the mold chips for the thin film model. To do this, the features fabricated from the edge of the mold will be measured and compared to that of the features in the middle of the mold. The features at the edge of the mold should fill less than the ones in the center, allowing the pressure distribution to be established.

The 5mm x 5mm chips will be used to determine the highest achievable aspect ratio and validate the nano-molding model. With the varied spacing and varied aspect ratios, the features created from these molds will also vary, allowing a limit curve of the achievable aspect ratios to be determined. This will then be compared to the theoretical model.

## CONCLUSIONS

Theoretical models to assess the thermoplastic molding process were developed. Also, new molds were created with high aspect ratio trench and hole features of varying dimensions and spacing. Finally a robust nanomolding process was implemented. With the new molds and process, the theoretical models that were developed will be compared to the experimental results.

## ACKNOWLEDGMENTS

Support from NSF (ECE #0425826) is gratefully acknowledged. Also, the authors appreciate the assistance from Dr. Todd Gross (UNH) for Atomic Force Microscope, and the Kostas Center for Nanomanufacturing at Northeastern University. Finally, the authors would like to thank Atakan



Peker (LiquidMetal Technologies Inc.) for providing the Vitreloy-1b material used.

## REFERENCES

1. Schroers, J. "The Superplastic Forming of Bulk Metallic Glasses", *Journal of Metals*, May 2005, pp. 35-39.
2. Bardt, J.A., Ziegert, J.C., Schmitz, T., Sawyer, W.G., and Bourne, G., "Precision Molding of Complex Metallic Micro-structures", *Proceedings of the International Conference on Micromanufacturing – ICOMM*, Urbana-Champaign, IL, Sept. 13-15, 2006, pp. 274-279.
3. Saotome, Y., K. Imai, S. Shioda, S. Shimizu, T. Zhang, and A. Inoue, "The Micro-Nanoformability of Pt-based Metallic Glass and the Nanoforming of Three-Dimensional Structures", *Intermetallics*, Vol. 10, 2002, pp. 1241-1247.
4. Rason, K. "Nanoscale Molding of Bulk Metallic Glass", University of New Hampshire, M.S. Thesis, September 2007.
5. Sachin, B. "Thin Film Deposition on Plastic Substrates using Silicon Nanoparticles and Laser Nanoforming", *Journal of Materials Science and Engineering B*, 2006, pp. 228-236.
6. LiquidMetal Technologies, Inc., [www.liquidmetal.com](http://www.liquidmetal.com)
7. R. Panton, *Incompressible Flow*, Wiley-Interscience 1984.
8. Rason, K., Kinsey B. "Nanoscale Molding of a Zirconium Based Bulk Metallic Glass", *ASME International Mechanical Engineering Conference and Exposition*, Nov. 2007.
9. Saotome, Y., Itoh, K., Zhang, T. and Inoue, A. "Superplastic Nanoforming of Pd-Based Amorphous Alloy," *Scripta Materialia*. 44, 2001, pp. 1541–1545.
10. Schroers, J., Pham, Q., Desai, A., "Thermoplastic Forming of Bulk Metallic Glass-A Technology for MEMS and Microstructure Fabrication", *Journal of Microelectromechanical Systems*, v16 N 2, April 2007 pp. 240-7.
11. Johnson, W. L. and Samwer K., "A Universal Criterion for Plastic Yielding of Metallic Glasses with a  $T=T_g/2=3$  Temperature Dependence", *Physical Review Letters*, 4 Nov 2005, 195501.
12. Kundig, A. Dommann, W.L. Johnson and P.J. Uggowitzer, "High Aspect Ratio Micro Mechanical Structures Made of Bulk Metallic Glass", *Material Science and Engineering A*, 2004, pp. 327-331.
13. Meng, Q. "Strong Liquid Behavior of Bulk Metallic Glass", *Journal of Alloys and Compounds*, 2007, pp. 191-196.